

# Thermal decomposition kinetics of some aromatic azomonoethers

## Part IV. Non-isothermal kinetics of 2-allyl-4-((4-(4-methylbenzyloxy)phenyl)diazenyl)phenol in *air flow*

A. Rotaru · Anca Moanță · Gina Popa ·  
P. Rotaru · E. Segal

ICTAC2008 Conference  
© Akadémiai Kiadó, Budapest, Hungary 2009

**Abstract** Thermal analysis of 2-allyl-4-((4-(4-methylbenzyloxy)phenyl)diazenyl)phenol dye was performed in *air flow*. The compound thermal behavior was investigated using TG, DTG and DSC techniques, under non-isothermal linear regime. Kinetic parameters of the two decomposition steps were obtained by means of multi-heating rates methods. Isoconversional methods (KAS and FWO), Invariant Kinetic Parameters method and Perez-Maqueda et al. criterion (by means of CR and FW equations) were used.

**Keywords** Azomonoether dyes · IKP method · “Model-free” kinetics · Perez-Maqueda et al. criterion · Thermal analysis

### Introduction

Dyes containing “azo” group in their molecules are of large interest from the point of view of possible applications. Thermal analysis and kinetic studies of thermal induced changes of new compounds designed for temperature-controlled applications are a real need and an advantageous pointer before trying to functionalize them [1, 2]. Part IV on the thermal behavior of some azomonoethers, aims to identify the physical and chemical transformations of 2-allyl-4-((4-(4-methylbenzyloxy)phenyl)diazenyl)phenol, related to non-isothermal increasing temperature regimes in *air flow* and the kinetic characteristics of the two decomposition steps occurring. Previous studies on the thermal stability of azoic dyes [3–5] and non-isothermal decomposition kinetics of such compounds [6–9] have also been reported.

For a single heterogeneous process under any non-isothermal regime, the reaction rate can be expressed by Eq. 1:

$$\frac{d\alpha}{dt} = A \cdot f(\alpha) \cdot e^{-\frac{E}{RT}} \quad (1)$$

where  $\alpha$  is the conversion degree,  $(d\alpha/dt)$  is the reaction rate,  $A$  is the pre-exponential factor (frequency factor),  $E$  is the activation energy,  $f(\alpha)$  is the differential conversion function and  $R$  is the universal gas constant. Recent papers have reported on the critical analysis of the single rate model-fitting methods [10–18], suggesting that their use would lead frequently to uncertain values of the activation parameters. The entire kinetic triplet  $\{E, A, f(\alpha)\}$  that describes a physical or chemical transformation may be evaluated by means of simple procedures like isoconversional methods as shown by Vyazovkin [19, 20], but only after supplementary use of compensation effect of apparent activation parameters. However, this is true only for single processes, as in [21, 22], when there do not exist overlapping processes. It is worth to

---

A. Rotaru (✉)

Laser Department, INFILPR-National Institute for Laser, Plasma and Radiation Physics, Bvd. Atomistilor, Nr. 409, Magurele, PO Box MG-16, RO-077125 Bucharest, Romania  
e-mail: andrei.rotaru@infilpr.ro

A. Moanță

Faculty of Chemistry, University of Craiova,  
Calea Bucuresti Str., Nr. 107 I, Craiova, Romania

G. Popa

School of Chemistry, University of St Andrews,  
North Haugh, KY16 9ST St Andrews, Fife, UK

P. Rotaru

Faculty of Physics, University of Craiova,  
A.I. Cuza Str. Nr. 13, Craiova, Romania

E. Segal

Faculty of Chemistry, University of Bucharest,  
Bvd. Regina Elisabeta Nr. 4-12, Bucharest, Romania

mention that the evaluation of isoconversional pre-exponential factors is constrained on the existence of constant compensation effect parameters. Therefore, it was concluded the need of using also more sophisticated kinetic methods (Invariant Kinetic Parameters method [23], Perez-Maqueda et al. criterion [24] or Malek criterion [25]), combined with isothermal, non-isothermal non-linear (i.e. modulated temperature [26]) or sample controlled thermal experiments [27, 28].

From the point of view of possible applications (for dye lasers [29, 30], plastic composite materials [31] or textiles industry [32]), azomonoethers are a large interest class of dyes. Materials' aspect and color modifications are due to the thermal-induced chemical degradation of organic dyes used. The present studied compound is one of the new potential organic azoetic dyes, having a high chemical stability and therefore required in several industries. In order to establish the thermochemical stability domain and the limits of such dyes use, the study of its thermal behavior is needed. It is also important to be known, for the technological processing of materials (that contain them) which may happen at higher temperatures. Apart from the used temperature regime in the technological processing of new materials, the knowledge of kinetic parameters is very important as universal characteristic. Predictions of thermal behaviors of a certain dye may be made in other temperature conditions, experimentally undone. Clues may be provided to those deciding the use of a certain dye or of another, as well as the possibility of predicting the appropriate temperature regimes needed in the technological process. The lifetime of the dyes under laser constant irradiation parameters, the decomposed dye percentage and the kinetic parameters may be used for a kind of average apparent temperature profile estimation.

## Experimental

The investigated compound was prepared by diazotation of commercially available 4-[(4-methylphenyl)methoxy]benzamine (from AsisChem) using sodium nitrate in the presence of hydrochloric acid followed by coupling with 2-allylphenol [33, 34]. Thermal stability (TG, DTG and DSC) measurements of 2-allyl-4-((4-(4-methylbenzyloxy)phenyl)diazenyl)phenol (Fig. 1) were carried out in *air flow* (150 mL min<sup>-1</sup>), under non-isothermal linear regimes. A horizontal Diamond Differential/Thermogravimetric Analyzer from Perkin-Elmer Instruments was used during the experiments. Air flow has been chose because most of the applications the dyes have are to be found in such conditions.

Samples from 0.8 to 1.2 mg, contained in Al<sub>2</sub>O<sub>3</sub> crucibles, were heated from room temperature to 800 °C, with the heating rates of: 2, 4, 6 and 8 K min<sup>-1</sup>.

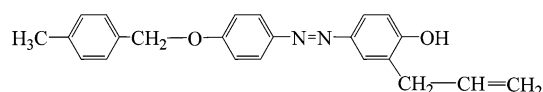


**Fig. 1** 2-Allyl-4-((4-(4-methylbenzyloxy)phenyl)diazenyl)phenol

## Results and discussion

### Thermal analysis

Figure 2 shows the thermoanalytical curves (TG, DTG, DTA and DSC) of 2-allyl-4-((4-(4-methylbenzyloxy)phenyl)diazenyl)phenol, recorded for 6 K min<sup>-1</sup>; similar curves were obtained for all other heating rates.

Before melting at 96 °C, a loss of approximately 6% that correspond to the remained toluene after synthesis may be noticed. The investigated compound decomposes in two steps. For the first step, a weak oxidative decomposition undergoes in the temperature range 150–290 °C. The experimental mass loss ( $\Delta m_{\text{exp}} = 73.68\%$ ) of the first step is very close to the theoretical mass loss ( $\Delta m_{\text{theor}} = 74.65\%$ ), which indicates the tropylium ion as remaining decomposition fragment—stable at those temperatures and in good agreement with the mass spectrometry results of such compounds [35–40]. The second decomposition step (350–600 °C) corresponds to the combustion of tropylium ions.

DSC thermal parameters of the thermal induced changes of the title compound, at 6 K min<sup>-1</sup> in *air flow*, are presented in Table 1.

### Kinetic analysis

The influence of different temperature regimes upon the thermal behavior of chemical compounds can provide kinetic parameters indicating change in the reaction pathway. The complexity of a stage can be expressed from the activation energy dependence on the conversion degree. This can be done using isoconversional methods for the evaluation of the activation energy. If *E* does not depend on

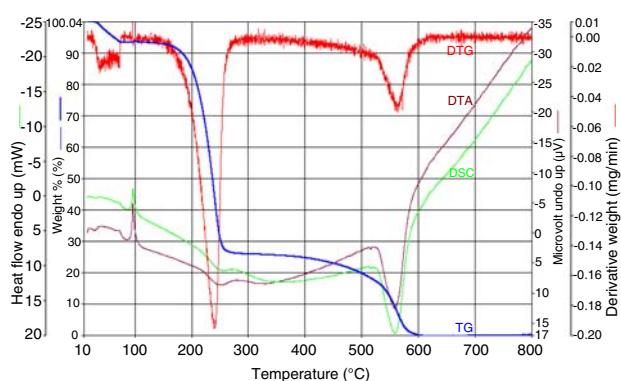


**Fig. 2** Thermoanalytical curves of 2-allyl-4-((4-(4-methylbenzyloxy)phenyl)diazenyl)phenol for 6 K min<sup>-1</sup> in air flow

**Table 1** DSC parameters for 2-allyl-4-((4-(4-methylbenzyloxy)phenyl)diazanyl)phenol changes at  $\beta = 6 \text{ K min}^{-1}$ 

Change	Thermal effect ( <i>Endo/Exo</i> )	Max. peak temp. $T_{\text{max}}/^{\circ}\text{C}$	Transferred heat $\Delta H/\text{kJ kg}^{-1}$
Melting	Endothermic	96	113.5
Oxidative decomposition	Exothermic	246	-371.9
Combustion	Exothermic	558	-4335.9

$\alpha$ , the investigated process is a simple one and should be described by a unique kinetic triplet. If  $E$  changes with  $\alpha$ , the process is complex [41]. Vyazovkin and co-workers [42, 43] established a algorithm for identifying the type of complex processes. When  $E$  increases with conversion degree, the process involves parallel reactions. When  $E$  decreases and the shape of its evolution is concave, then the process has reversible stages. For decreasing convex shape, the process changes the limiting stage. In order to discriminate between the occurring reactions, automatic programs were developed, assuming that the overall reaction is the sum of individual reaction steps [44–46].

### Isoconversional methods

The isoconversional procedures (“model-free” kinetics) can be classified as linear (the activation energy is evaluated from the slope of a straight line) and non-linear (the activation energy is evaluated from a specific minimum condition). The isoconversional integral linear methods are based on the following integral form of the reaction rate:

$$g(\alpha) = \int_0^{\alpha} \frac{d\alpha}{f(\alpha)} = \frac{A}{\beta} \int_0^{T_{\alpha}} e^{-\frac{E}{RT}} dT = \frac{A}{\beta} I(E_{\alpha}, T_{\alpha}) \quad (2)$$

where  $\beta$  is the heating rate,  $g(\alpha)$  is the integral conversion function and  $I(E_{\alpha}, T_{\alpha})$  represents the temperature integral. In our paper we make use of Kissinger–Akahira–Sunose (KAS method)—integral linear method [47, 48] and Flynn–Wall–Ozawa (FWO method)—integral linear method [49, 50].

Substitution of  $I(E_{\alpha}, T_{\alpha})$  in the Eq. 2 with Coats–Redfern approximation [51]:  $I(E_{\alpha}, T_{\alpha}) = \frac{RT_{\alpha}^2}{E_{\alpha}} e^{-\frac{E_{\alpha}}{RT_{\alpha}}}$ , gives Eq. 3—used by KAS method:

$$\ln \frac{\beta}{T^2} = \ln \frac{AR}{Eg(\alpha)} - \frac{E}{RT} \quad (3)$$

Similar substitution with Doyle approximation [52]:  $I(E_{\alpha}, T_{\alpha}) = \frac{E_{\alpha}}{R} e^{(-5.331 - 1.052 \frac{E_{\alpha}}{RT_{\alpha}})}$ , gives Eq. 4—used by FWO method:

$$\ln \beta = \ln \frac{AE}{Rg(\alpha)} - 5.331 - 1.052 \frac{E}{RT} \quad (4)$$

Thus, for  $\alpha = \text{const.}$ , the plot  $\ln(\beta/T^2)$  versus  $(1/T)$  or  $\ln(\beta)$  versus  $(1/T)$ , obtained from the experimental thermogravimetric curves recorded for several constant-heating

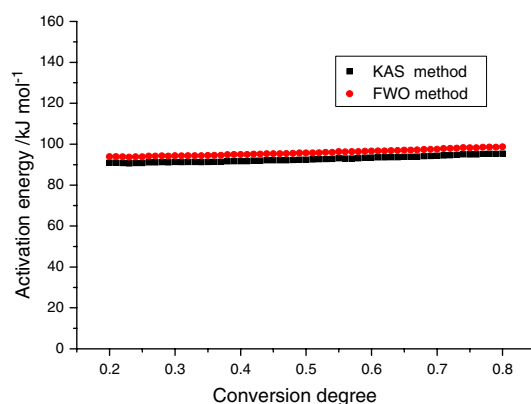


**Fig. 3** Isoconversional activation energy of the non-isothermal oxidative decomposition of 2-allyl-4-((4-(4-methylbenzyloxy)phenyl)diazanyl)phenol in *air flow* (step 1)

rates, should be a straight line whose slope could be used for the activation energy evaluation.

Figure 3 shows the kinetic results of the first decomposition step, obtained using KAS and FWO methods, as values of the activation energy for various conversion degrees from 0.2 to 0.8 with a step of 0.01, using our TKS program (SP 1.0 version) [53].

During the first decomposition step, the activation energy remains practically constant, describing a single reaction; the accuracy in determining the activation energy is very high—over 0.99690.

The mean values of the activation energy for  $0.2 < \alpha < 0.8$  are:

$$\bar{E}_{\text{KAS}} = 92.7 \pm 1.6 \text{ kJ mol}^{-1} \quad \bar{E}_{\text{FWO}} = 95.9 \pm 1.7 \text{ kJ mol}^{-1}$$

The results obtained by KAS and FWO methods are comparable. The differences between the values of the activation energy obtained using these two isoconversional integral methods may be attributed to the different approximations of the temperature integral they use. Even if some authors consider useless to perform calculations by means of FWO method (considered to be one of the worst), it may help, however, to know the limits the activation energy is to be found.

For the second decomposition step (combustion of tropylium ion), the isoconversional activation energy is shown in Fig. 4.

Because during the second step no condensed compound forms, the activation energy decreases with the consumption

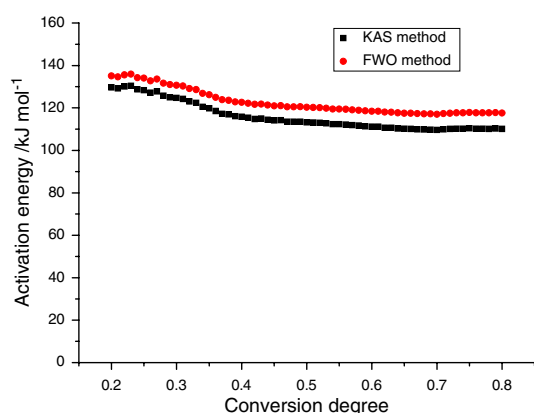


**Fig. 4** Isoconversional activation energy of the non-isothermal combustion of tropylium ion in air flow (step 2)

of the reaction. Since it has no well-defined shape (not concave nor convex), but obtained with reliable correlation coefficients (more than 0.9930), it is not possible to establish the kinetic model or reaction type. It is likely that during the first decomposition step, tropylium-based residues formed; comparing with thermal decomposition of [4-(4-chlorobenzoyloxy)-3-methylphenyl](*p*-tolyl)diazene [54], where for the first step  $\bar{E}_{KAS}$  is much higher ( $176.6 \text{ kJ mol}^{-1}$ ) than in this case ( $92.7 \text{ kJ mol}^{-1}$ ), other macromolecules forming each time. The difference in activation energies may explain the obtaining of some raw product (percentages indicating at such temperatures the tropylium ions), but instead, the formation of different residues (based on tropylium fragments). Higher values of the activation energies induce the formation of better assembled molecules. Stronger bonds develop higher activation energies (at  $\alpha = 0.5$ ,  $117 \text{ kJ mol}^{-1}$  in this case, instead of  $150 \text{ kJ mol}^{-1}$ ) for the combustion of the tropylium-based residues. The two curves are of different values, but almost equidistant one to the other, suggesting the same type of chemical decomposition behavior.

#### Invariant kinetic parameters (IKP) method

Based on Criado and Morales early observation [55], that almost any  $\alpha = \alpha(T)$  or  $(d\alpha/dt) = (d\alpha/dt)(T)$  experimental curve may be correctly described by several conversion

functions, the use of an integral or differential model-fitting method leads to different values of the activation parameters. Although being obtained with high accuracy, the values change with different heating rates and among conversion functions. In the present paper, the chosen model-fitting methods were Coats–Redfern [51] and Flynn–Wall [49]. The apparent activation parameters of the first decomposition step, obtained for each heating rate of the best-fitting kinetic models are presented in Table 2 (when applying the CR equation). Similar results have been obtained when applying FW equation.

The straight lines  $\ln A_\beta$  versus  $E_\beta$  for several constant-heating rates should intersect in a point (isoparametric point [56]) that corresponds to the true values of the activation energy and pre-exponential factor. They were named invariant kinetic parameters ( $E_{inv}$ ,  $A_{inv}$ ).

The apparent kinetic parameters of the first thermal decomposition step, of 2-allyl-4-((4-(4-methylbenzyl-oxy)phenyl)diazanyl)phenol, in air flow, are represented in  $\ln A$  versus  $E$  space (Fig. 5—by CR equation).

Certain variations of the experimental conditions, as well as the straight lines (corresponding to different heating rates) junction at low values, determine a region of intersection rather than a unique point in the  $\ln A$  versus  $E$  plot. The detailed image in Fig. 5—undersized figure in the up-left corner shows the non-convergent straight-lines and the

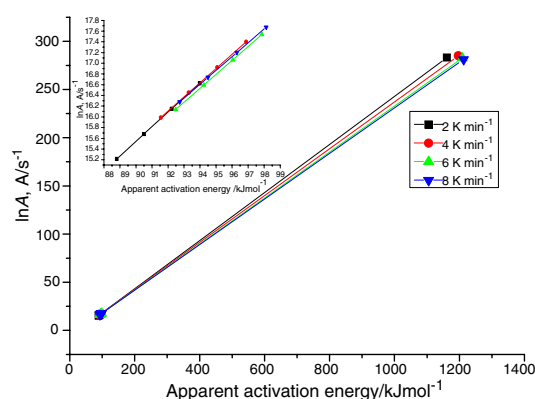


**Fig. 5**  $\ln A$  versus  $E$  space of all best-fitting kinetic models, by CR equation

**Table 2** Apparent activation parameters by Coats–Redfern equation for each applied heating rate

Kinetic model	2 K min <sup>-1</sup>			4 K min <sup>-1</sup>			6 K min <sup>-1</sup>			8 K min <sup>-1</sup>		
	$E$ (kJ mol <sup>-1</sup> )	$\ln A$ (A/s <sup>-1</sup> )	$r$	$E$ (kJ mol <sup>-1</sup> )	$\ln A$ (A/s <sup>-1</sup> )	$r$	$E$ (kJ mol <sup>-1</sup> )	$\ln A$ (A/s <sup>-1</sup> )	$r$	$E$ (kJ mol <sup>-1</sup> )	$\ln A$ (A/s <sup>-1</sup> )	$r$
F0.45	88.8	15.21	0.99996	91.5	15.98	0.99997	92.5	16.13	0.99999	92.7	16.28	1
F0.50	90.5	15.68	0.99999	93.3	16.45	0.99998	94.2	16.59	0.99995	94.5	16.73	0.99998
F0.55	92.2	16.15	0.99999	95.1	16.92	0.99997	96.0	17.06	0.99989	96.3	17.20	0.99994
F0.60	94.0	16.62	0.99997	96.9	17.40	0.99994	97.9	17.53	0.99981	98.1	17.67	0.99988
A0.1	1161.2	283.26	0.99905	1196.5	285.05	0.99892	1209.1	282.53	0.99848	1213.1	281.23	0.99868

**Table 3** Compensation effect parameters for all selected kinetic models by CR and FW equations

ASKM $\beta$ (K min <sup>-1</sup> )	CR equation			FW equation		
	$a_\beta$ (A/s <sup>-1</sup> )	$b_\beta$ (mol J <sup>-1</sup> )	$r$	$a_\beta$ (A/s <sup>-1</sup> )	$b_\beta$ (mol J <sup>-1</sup> )	$r$
2	-6.91791	$2.499 \times 10^{-4}$	0.99998	-7.40625	$2.579 \times 10^{-4}$	0.99999
4	-6.24377	$2.434 \times 10^{-4}$	0.99997	-6.74373	$2.513 \times 10^{-4}$	0.99998
6	-5.86453	$2.385 \times 10^{-4}$	0.99997	-6.34396	$2.462 \times 10^{-4}$	0.99999
8	-5.58681	$2.364 \times 10^{-4}$	0.99998	-6.05497	$2.440 \times 10^{-4}$	0.99998

values for the  $F_n$  models. Lesnikovich and Levchik suggested that correlating these values by the apparent compensation effect:  $\ln A = a_\beta + b_\beta E$ , one obtains the compensation effect parameters,  $a_\beta$  and  $b_\beta$  (Table 3) which strongly depend on the heating rate ( $\beta$ ) as well as on the considered set of conversion functions [23]. Therefore, the evaluation of the invariant kinetic parameters must be performed using the supercorrelation equation:

$$a_\beta = \ln A_{\text{inv}} - b_\beta \cdot E_{\text{inv}} \quad (5)$$

The plot of  $a_\beta$  versus  $b_\beta$ , obtained for several constant-heating rates, is a straight line whose parameters allow the determination of  $\ln A_{\text{inv}}$  and  $E_{\text{inv}}$ .

It is easy to notice from Fig. 5 that  $F_n$  functions (for  $n = 0.45 - 0.60$ ) are the most adequate, because the intersection is around  $95 \pm 10$  kJ mol<sup>-1</sup>. Good results were obtained also for the diffusion functions, but as it was previously shown [57, 58] in such cases (liquid state decomposition), the contribution of diffusion functions is less probable, they even providing increased errors. The efficiency of IKP method is one more time revealed, when introducing other kinetic models, each of them with their very different apparent values. When introducing A0.1 between the selected models, the overall values deriving from the single-heating rate straight lines remaining unchanged (detail in Fig. 5).

For all selected kinetic models (ASKM), the invariant kinetic parameters, obtained using the compensation effect parameters are presented in Table 4.

Both equations provide close results; the 2 kJ mol<sup>-1</sup> difference is the consequence of the many values involved in calculations.

For the second step, the use of IKP method is not possible since the isoconversional activation energy varies and therefore no convergence will be obtained when gathering the results of *single-heating rate methods*.

**Table 4** Invariant kinetic parameters for all selected kinetic models by CR and FW equations

IKP for ASKM	$E_{\text{inv}}$ (kJ mol <sup>-1</sup> )	$\ln A_{\text{inv}}$ (A/s <sup>-1</sup> )	$r_{\text{inv}}$
CR equation	96.0	17.101	0.99752
FW equation	94.1	16.873	0.99771

### Perez-Maqueda et al. criterion

In order to obtain the appropriate kinetic equation (for step 1), one can discriminate between the set of best-fitting conversion functions by applying the Perez-Maqueda et al. criterion [24]. Even if model-fitting methods and IKP method select a group of presumable conversion functions, they cannot precisely establish the right and unique model from a type of kinetic models (i.e. in our case, all possibilities of  $F_n$  type models, with  $n = 0.45 - 0.60$ ).

According to Perez-Maqueda et al. criterion, the correct kinetic model corresponds to the independence of the activation parameters on the heating rate. By applying any differential or integral model-fitting method, for every constant heating rate, the true kinetic model shall provide both the same constant activation energy as well as the pre-exponential factor.

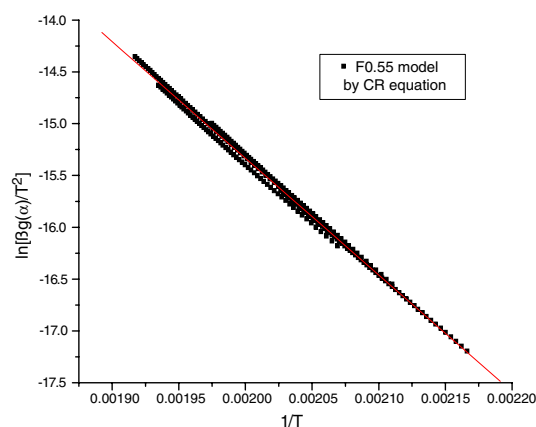
If Coats-Redfern equation written in the form:

$$\ln \frac{\beta g(x)}{T^2} = \ln \frac{AR}{E} - \frac{E}{RT} \quad (6)$$

or Flynn-Wall equation written as:

$$\ln[\beta \cdot g(x)] + 5.331 = \ln \frac{AE}{R} - 1.052 \frac{E}{RT} \quad (7)$$

are used, for the correct conversion function, all the points  $\{\ln[\beta g(x)/T^2]$  vs.  $1/T\}$  (Fig. 6 in CR plot) and

**Fig. 6** Perez-Maqueda et al. straight lines for all constant-heating rates, by CR equation

**Table 5** Perez-Maqueda et al. kinetic parameters using CR and FW rewritten equations for  $F_{0.55}$ 

$F_{0.55}$ kinetic model	$E$ (kJ mol <sup>-1</sup> )	$\ln A$ (A/s <sup>-1</sup> )	$r$
CR equation	93.6	16.514	0.99840
FW equation	96.8	17.565	0.99838

$\{\ln[\beta g(x)] + 5.331$  vs.  $1/T\}$  (for FW plot) corresponding to all applied heating rates lie on the same straight line.

The best overlapping of the  $\{\ln[\beta g(x)/T^2]$  vs.  $1/T\}$  (in CR plot) and  $\{\ln[\beta g(x)] + 5.331$  vs.  $1/T\}$  (in FW plot) points, corresponding to all applied heating rates was obtained for  $F_{0.55}$  kinetic model. The kinetic parameters according to Perez-Maqueda et al. criterion are presented in Table 5:

Although  $F_{0.50}$ , also known as R2 (contracting area, i.e. bidimensional shape) model, was found to be one of the most frequent kinetic model describing thermal induced decompositions of liquid systems [59, 60],  $F_{0.55}$  equation applies in this case of a linear compound decomposition and formation of planar tropylium-based residues.

## Conclusions

Thermal analysis of 2-allyl-4-((4-(4-methylbenzyloxy)phenyl)diazenyl)phenol dye was performed in *air flow*. After melting at 96 °C, an oxidative decomposition undergoes in the temperature range 150–290 °C. This is followed by the combustion of tropylium ions between 350 and 600 °C. Kinetic parameters of the first decomposition step were evaluated by means of multi-heating rates methods, such as isoconversional (KAS and FWO) methods, IKP method and Perez-Maqueda et al. criterion. The selection of different kinetic models ( $F_n$ ,  $n = 0.45 - 0.60$  and A0.1) leads finally to invariant kinetic parameters in the region of low reaction order models, and close to the isoconversional activation energies ( $\sim 95 \pm 1$  kJ mol<sup>-1</sup>). The use of Perez-Maqueda et al. criterion confirmed the 10<sup>7</sup> order of pre-exponential factor (similar to the invariant pre-exponential factor) and point towards  $F_{0.55}$  as the unique and right kinetic model of the first decomposition step of 2-allyl-4-((4-(4-methylbenzyloxy)phenyl)diazenyl)phenol. The paper provides information on the kinetic characteristics of the thermo-oxidative decomposition of 2-allyl-4-((4-(4-methylbenzyloxy)phenyl)diazenyl)phenol, useful for several industries (composite plastic materials, textiles and laser dyes).

Comparing the activation energies for the combustion of the obtained tropylium-based residues with others obtained in [54], one have observed the same trend and thus concluded on bonding strengths.

**Acknowledgements** The authors are grateful to Dr. S. Chercheja for the fruitful discussions.

## References

- Rotaru A, Constantinescu C, Rotaru P, Moanta A, Dumitru M, Socaciu M, et al. Thermal analysis and thin films deposition by matrix assisted pulsed laser evaporation of a 4CN type azomonoether. *J Therm Anal Calorim.* 2008;92:279–84.
- Chao T-Y, Chang H-L, Su W-C, Wu J-Y, Jeng R-J. Nonlinear optical polyimide/montmorillonite nanocomposites consisting of azobenzene dyes. *Dye Pigment.* 2008;77:515–24.
- Dincalp H, Toker F, Durucasu J, Avciyasi N, Icli S. New thiophene-based azo ligands containing azo methine group in the main chain for the determination of copper(II) ions. *Dye Pigment.* 2007;75:11–24.
- Gür M, Kocaokutgen H, Taş M. Synthesis, spectral, and thermal characterisations of some azo-ester derivatives containing a 4-acryloyloxy group. *Dye Pigment.* 2007;72:101–8.
- Badea M, Emandi A, Marinescu D, Cristurean E, Olar R, Braileanu A, et al. Thermal stability of some azo-derivatives and their complexes. *J Therm Anal Calorim.* 2003;72:525–31.
- Rotaru A, Moanta A, Sălăgeanu I, Budrugaec P, Segal E. Thermal decomposition kinetics of some aromatic azomonoethers. Part I: Decomposition of 4-[(4-chlorobenzyl)oxy]-4'-nitro-azobenzene. *J Therm Anal Calorim.* 2007;87:395–400.
- Rotaru A, Jurca B, Moanta A, Salageanu I, Segal E. Kinetic study of the thermal decomposition of some aromatic ortho-chlorinated azomonoethers. I. Decomposition of 4-[(2-chlorobenzyl)oxi]-4'-trifluoromethyl-azobenzene. *Rev Roum Chim.* 2006;51:373–8.
- Chen Z, Wu Y, Gu D, Gan F. Nickel(II) and copper(II) complexes containing 2-(2-(5-substitued isoxazol-3-yl)hydrazono)-5,5-dimethylcyclohexane-1,3-dione ligands: synthesis, spectral and thermal characterizations. *Dye Pigment.* 2008;76:624–31.
- Rotaru A, Kropidowska A, Moanță A, Rotaru P, Segal E. Thermal decomposition kinetics of some aromatic azomonoethers. Part II: Non-isothermal study of three liquid crystals in dynamic air atmosphere. *J Therm Anal Calorim.* 2008;92:233–8.
- Tanaka H, Brown ME. The theory and practice of thermoanalytical kinetics of solid-state reactions. *J Therm Anal Calorim.* 2005;80:795–7.
- Maciejewski M, Vyazovkin S. Comments on “The use of MoO<sub>3</sub> and NiO (pure or mixed) oxide catalysts in the decomposition of KMnO<sub>4</sub>” by S.A. Halawy and M.A. Mohamed. *Thermochim Acta.* 2001;370:149–54.
- Budrugaec P, Segal E, Pérez-Maqueda LA, Criado JM. The use of the IKP method for evaluating the kinetic parameters and the conversion function of the thermal dehydrochlorination of PVC from non-isothermal data. *Polym Degrad Stab.* 2004;84:311–20.
- Brown ME, Maciejewski M, Vyazovkin S, Nomen R, Sempere J, Burnham AK, et al. Computational aspects of kinetic analysis. Part A: The ICTAC kinetics project—data, methods and results. *Thermochim Acta.* 2000;355:125–43.
- Roduit B. Computational aspects of kinetic analysis. Part E: The ICTAC Kinetics Project—numerical techniques and kinetics of solid state processes. *Thermochim Acta.* 2000;355:171–80.
- Vyazovkin S. Computational aspects of kinetic analysis. Part C: The ICTAC Kinetics Project—the light at the end of the tunnel? *Thermochim Acta.* 2000;355:155–63.
- Maciejewski M. Computational aspects of kinetic analysis. Part B: The ICTAC Kinetics Project—the decomposition kinetics of calcium carbonate revisited, or some tips on survival in the kinetic minefield. *Thermochim Acta.* 2000;355:145–54.

17. Burnham AK. Computational aspects of kinetic analysis. Part D: The ICTAC kinetics project—multi-thermal—history model-fitting methods and their relation to isoconversional methods. *Thermochim Acta*. 2000;355:165–70.
18. Vyazovkin S. Model-free kinetics. Staying free of multiplying entities without necessity. *J Therm Anal Calorim*. 2006;83:45–51.
19. Vyazovkin S. A unified approach to kinetic processing of non-isothermal data. *Int J Chem Kinet*. 1996;28:95–101.
20. Vyazovkin S. Isoconversional kinetics. In: Brown ME, Gallagher PK, editors. *The handbook of thermal analysis and calorimetry*, Chap 13, vol. 5: Recent advances, techniques and applications. Amsterdam: Elsevier; 2008. 503 pp.
21. Zhou DL, Schmitt EA, Zhang GGZ, Law D, Wight CA, Vyazovkin S, et al. Model-free treatment of the dehydration kinetics of nedocromil sodium trihydrate. *J Pharm Sci*. 2003;92:1367–76.
22. Zhou DL, Schmitt EA, Zhang GG, Law D, Vyazovkin S, Wight CA, et al. Crystallization kinetics of amorphous nifedipine studied by model-fitting and model-free approaches. *J Pharm Sci*. 2003;92:1779–92.
23. Lesnikovich AI, Levchik SV. A method of finding invariant values of kinetic parameters. *J Therm Anal*. 1983;27:89–93.
24. Perez-Maqueda LA, Criado JM, Gotor FJ, Malek J. Advantages of combined kinetic analysis of experimental data obtained under any heating profile. *J Phys Chem A*. 2002;106:2862–8.
25. Malek J. Kinetic analysis of crystallization processes in amorphous materials. *Thermochim Acta*. 2000;355:239–53.
26. Gill PS, Sauerbrunn SR, Reading M. Modulated differential scanning calorimetry. *J Therm Anal*. 1993;40:931–9.
27. Sorensen OT. Quasi-isothermal methods in thermal analysis. *Thermochim Acta*. 1981;50:163–75.
28. Rouquerol J. L'analyse thermique a vitesse de decomposition constante. *J Therm Anal*. 1970;2:123–40.
29. Lu M, Cunningham BT, Park SJ, Eden JG. Vertically emitting, dye-doped polymer laser in the green ( $\lambda \sim 536$  nm) with a second order distributed feedback grating fabricated by replica molding. *Opt Commun*. 2008;281:3159–62.
30. He BQ, Liao Q, Huang Y. Random lasing in a dye doped cholesteric liquid crystal polymer solution. *Opt Mater*. 2008;31:375–9.
31. Yamaguchi T, Tobe N, Matsumoto D, Arakawa H. Highly efficient plastic substrate dye-sensitized solar cells using a compression method for preparation of TiO<sub>2</sub> photoelectrodes. *Chem Commun*. 2007;45:4767–9.
32. Holme I. Recent developments in colorants for textile applications. *Surf Coat Int B Coat Trans*. 2002;85:243–64.
33. Haghbeen K, Tan EW. Facile synthesis of catechol azo dyes. *J Org Chem*. 1998;63:4503–5.
34. Odabasoglu M, Turgut G, Icbudak H. Preparation and characterization of chromophore group containing cyclotriphosphazenes: IV. Spectroscopic and thermal investigation of some hexakis (*p*-phenylazo-*o*-allylphenoxy)cyclotriphosphazenes. *J Mol Struct*. 2004;691:249–57.
35. Ozdilek C, Toppare L, Yagci Y, Hacialoglu J. Characterization of polypyrrole/polytetrahydrofuran graft copolymers by direct pyrolysis mass spectrometry. *J Anal Appl Pyrol*. 2002;64:363–78.
36. Moanta A, Florea S. New phenoxyacetic acid analogues with antimicrobial activity. *Rev Chim*. 2008;59:708–11.
37. Radu S. Electron impact mass spectrometry of aromatic azoethers. *Eur Mass Spectrom*. 1995;1:561–72.
38. Gilland JC, Lewis JS. Mass-spectroscopy of 4-amino-4'-nitroazobenzene compounds. *Org Mass Spectrom*. 1974;9:1148–53.
39. Messmer K, Nuyken O. Mass spectroscopic investigation of azo-compounds. 1. *Org Mass Spectrom*. 1977;12:100–5.
40. Bratulescu G. Mass spectra of aromatic azoethers and azoxyethers. *Rev Roum Chim*. 2000;45:277–83.
41. Budrugaec P. Some methodological problems concerning the kinetic analysis of non-isothermal data for thermal and thermo-oxidative degradation of polymers and polymeric materials. *Polym Degrad Stab*. 2005;89:265–73.
42. Vyazovkin S, Lesnikovich AI. An approach to the solution of the inverse kinetic problem in the case of complex processes. Part I: Methods employing a series of thermoanalytical curves. *Thermochim Acta*. 1990;165:273–80.
43. Vyazovkin S, Sbirrazzuoli N. Isoconversional kinetic analysis of thermally stimulated processes in polymers. *Macromol Rapid Commun*. 2006;27:1515–32.
44. Opfermann JR, Hädrich W. Prediction of the thermal response of hazardous materials during storage using an improved technique. *Thermochim Acta*. 1995;263:29–50.
45. Opfermann JR. Kinetic analysis using multivariate non-linear regression. I. Basic concepts. *J Therm Anal Calorim*. 2000;60:641–58.
46. Opfermann JR, Kaisersberger E, Flammersheim HJ. Model-free analysis of thermoanalytical data—advantages and limitations. *Thermochim Acta*. 2002;391:119–27.
47. Kissinger HE. Reaction kinetics in differential thermal analysis. *Anal Chem*. 1957;29:1702–6.
48. Akahira T, Sunose T. (Trans. 1969) Joint convention of four electrical institutes. Paper no. 246. *Res Rep Chiba Inst Technol*. 1971;16:22–31.
49. Flynn JH, Wall LA. General treatment of thermogravimetry of polymers. *J Res Natl Bur Stand A*. 1966;70:487–523.
50. Ozawa T. A new method of analysing thermogravimetric data. *Bull Chem Soc Jpn*. 1965;38:1881–6.
51. Coats AW, Redfern JP. Kinetic parameters from thermogravimetric data. *Nature*. 1964;201:68–9.
52. Doyle CD. Kinetic analysis of thermogravimetric data. *J Appl Polym Sci*. 1962;5:285–92.
53. Rotaru A, Gosa M, Rotaru P. Computational thermal and kinetic analysis software for non-isothermal kinetics by standard procedure. *J Therm Anal Calorim*. 2008;94:367–71.
54. Rotaru A, Bratulescu G, Rotaru P. Thermal analysis of azoic dyes: Part I. Non-isothermal decomposition kinetics of [4-(4-chlorobenzoyloxy)-3-methylphenyl](*p*-tolyl)diazene in dynamic air atmosphere. *Thermochim Acta*. 2009;489:63–9.
55. Criado JM, Morales J. Defects of thermogravimetric analysis for discerning between first order reactions and those taking place through the Avrami-Erofeev's mechanism. *Thermochim Acta*. 1976;16:382–7.
56. Vyazovkin S, Lesnikovich AI. Estimation of the pre-exponential factor in the isoconversional calculation of effective kinetic parameters. *Thermochim Acta*. 1988;128:297–300.
57. Budrugaec P. The Kissinger law and the IKP method for evaluating the non-isothermal kinetic parameters. *J Therm Anal Calorim*. 2007;89:143–51.
58. Budrugaec P, Segal E. Applicability of the Kissinger equation in thermal analysis (revisited). *J Therm Anal Calorim*. 2007;88:703–8.
59. Dong Z, Salisbury JS, Zhou D, Munson E, Schroeder SA, Prakash J, et al. Dehydration kinetics of neotame monohydrate. *J Pharm Sci*. 2002;91:1423–31.
60. Rotaru A, Moanta A, Rotaru P, Segal E. Thermal decomposition kinetics of some aromatic azomonoethers: Part III. Non-isothermal study of 4-[(4-chlorobenzyl)oxy]-4'-chloroazobenzene in dynamic air atmosphere. *J Therm Anal Calorim*. 2009;95:161–6.